PHYSICAL REVIEW E VOLUME 62, NUMBER 5 NOVEMBER 2000

Correlation between the Kolmogorov-Sinai entropy and the self-diffusion coefficient in simple liquids

Hyunsoo Pang, Young-han Shin, Dongchul Ihm, and Eok Kyun Lee*
Department of Chemistry and School of Molecular Science (BK21), Korea Advanced Institute of Science and Technology,
373-1, Gusongdong, Yuseongku, Taejon, Korea

Oyeon Kum
Institute for Shock Physics, Washington State University, Pullman 99164, Washington

(Received 28 January 2000; revised manuscript received 11 May 2000)

Molecular dynamics simulations were performed for soft- and hard-sphere systems, for number densities ranging from 0.5 to 1.0, and the Kolmogorov-Sinai entropy (KS entropy) and self-diffusion coefficients were calculated. It is found that the KS entropy, when expressed in terms of average collision frequency, is uniquely related to the self-diffusion coefficient by a simple scaling law. The dependence of the KS entropy on average collision frequency and number density was also explored. Numerical results show that the scaling laws proposed by Dzugutov, and by Beijeren, Dorfman, Posch, and Dellago, can be applied to both soft- and hard-sphere systems by changing to more generalized forms.

PACS number(s): 61.20.Ja, 05.45.−a, 05.70.Ce

I. INTRODUCTION

Studies by Hoover, Posch, and co-workers [1–4] pioneered the numerical calculation of Lyapunov exponents for molecular dynamics simulation. The Lyapunov spectra, which provide useful information characterizing the degree of chaos present in dynamical systems, have been extensively investigated for simple fluids through numerical and theoretical studies. Progress has been made to the point that the second law of thermodynamics and macroscopic irreversibility can be explained with these quantities [5]. Furthermore, their relations to the transport coefficients or the thermodynamic entropy in the condensed phase are now an important issue [6]. In an intriguing paper by Dzugutov [7], the self-diffusion coefficient in simple atomic condensed systems, expressed in terms of the frequency of atomic collisions, was shown to be related to thermodynamic entropy by a universal scaling law. In later studies, Dzugutov, Aurell, and Vulpiani [8] numerically examined the connection between the Kolmogorov-Sinai (KS) entropy and the thermodynamic excess entropy obtained by the thermodynamic integration method; the authors found that there exists a linear relationship between these two quantities. However, the thermodynamic entropy obtained by Dzugutov in Ref. [7], which is restricted to the two-particle approximation, showed a large deviation from that obtained by the thermodynamic integration method. It should be noted that the values of excess entropy restricted to the two-particle approximation are not reliable in dense fluids. Moreover, the numerical values of the self-diffusion coefficients do not seem to be consistent with those proposed by Speedy [9] or Erpenbeck and Wood [10].

Since the basic underlying dynamical processes of diffusion are collisions between particles with convex potential surfaces, the phase-space trajectory is highly unstable due to its sensitive dependence on the initial conditions. This phenomenon is characterized in terms of the set of Lyapunov exponents λ_l ($l=1,\ldots,6N$), usually ordered from largest to smallest. KS entropy is a measurement of the time rate of information loss as a chaotic phase-space trajectory evolves in phase space. Since KS entropy has the dimensionality of inverse time, its description requires a universal time scale. The most natural time scale in atomic dynamics is the average collision frequency ν, which can be defined in a system of hard spheres as

$$\nu=4\rho\sigma^2\left(\frac{\pi k_B T}{m}\right)^{1/2} g(\sigma), \tag{1}$$

where σ the is effective atomic diameter and ρ is the number density defined as $\rho=N/V$ [11]. For the case of a soft potential we define σ as the position of the first maximum of the pair correlation function $g(r)$. In this study, we examine the relationship between the values of the KS entropy and the self-diffusion coefficient D for soft- and hard-sphere fluids, respectively, for various number densities ρ ranging from 1.0 to 0.5; this essentially includes the entire liquid regime up to near solidification. In Sec. II we briefly describe the numerical methods for the evaluation of the time evolution of many-body systems in phase space and in tangent space. In Sec. III we present our results and discuss the behavior of D with respect to h_{KS}, in addition to the relation between h_{KS} and the average collision frequency ν. Our conclusions follow in Sec. IV.

II. DESCRIPTION OF THE MODEL

Simulations were performed for three-dimensional classical systems consisting of N identical particles with mass m in a volume V with periodic boundary conditions. Then, the equations of motion for the state vector $\mathbf{\Gamma}(t)$ were conveniently written as an autonomous system of first-order differential equations by

$$\dot{\mathbf{\Gamma}}(t)=\mathbf{G}(\mathbf{\Gamma}(t)), \tag{2}$$

---

*Author to whom correspondence should be addressed.

where

$$\boldsymbol{\Gamma}(t) = (\boldsymbol{r}_1(t), \boldsymbol{r}_2(t), \ldots, \boldsymbol{r}_N(t), \boldsymbol{p}_1(t), \boldsymbol{p}_2(t), \ldots, \boldsymbol{p}_N(t)).$$

For a system with continuous interaction potential, we used a short-range purely repulsive soft potential with the form

$$V(r) = 4\epsilon\left[\left(\frac{\sigma'}{r}\right)^{2n_g} - \left(\frac{\sigma'}{r}\right)^{n_g}\right] + \epsilon, \tag{3}$$

which has no second derivative at the cutoff distance $2^{1/n_g}\sigma'$. The Weeks-Chandler-Anderson (WCA) potential corresponds to $n_g = 6$. Throughout this paper we have used the usual reduced units: distance made dimensionless by dividing by σ', energy and temperature made dimensionless by dividing by the characteristic interaction energy ϵ defined in Eq. (3), and time made dimensionless by dividing by $(m\sigma^2/\epsilon)^{1/2}$. The equations of motion are integrated with a fourth-order Runge-Kutta algorithm with a time step $\Delta t = 0.001$. The initial temperature was set sufficiently high to obtain a random configuration; then velocities were repeatedly scaled to adjust to the required temperature within a 1% deviation. Once the required temperature was obtained, iterations over 2×10^5 time steps were performed to reach equilibrium. After equilibrium was obtained, we iterated for 1×10^6 time steps corresponding to 10^3 time units to evaluate static and dynamic properties. Energy was conserved with an accuracy of one part in 10^5 over an entire run of typically 10^3 time units.

On the other hand, for hard-sphere systems the equations of motion are no longer written as a continuous form. Between collisions, the particles move in a straight line; whenever two particles collide, the smooth streaming is interrupted by elastic collisions which are discontinuous events. This can be represented by the following discrete map:

$$\boldsymbol{\Gamma}^f = F(\boldsymbol{\Gamma}^i), \tag{4}$$

where the superscripts i and f indicate the initial and final states of map F specifying the action of instantaneous events on phase vector $\boldsymbol{\Gamma}$. F is differentiable with respect to the phase-space coordinates.

To calculate the Lyapunov spectra, we consider a bundle of trajectories that start at infinitesimally nearby points in phase space, with each trajectory in the bundle denoted by $\boldsymbol{\Gamma}(0) + \boldsymbol{\delta}_l(0)$ for some infinitesimal $\boldsymbol{\delta}_l(0)$ $(l = 1, \ldots, N)$. The time rate of separation for this trajectory bundle in various directions perpendicular to the direction flow, if exponential, is characterized by a set of nonzero Lyapunov exponents that are positive in expanding directions and negative in contracting ones. According to Oseledec [12], there are $6N$ orthogonal initial vectors yielding a set of exponents referred to as the Lyapunov spectrum of the system. These exponents are independent of metric and initial conditions. In a Hamiltonian system, phase volume is conserved, and certain directions must be exactly compensated for by contraction in other directions. Furthermore, due to the symplectic nature of the equations of motion, the Lyapunov exponents appear in pairs of equal magnitude and opposite signs. In a system of $6N$ dimensions, the conservations of total energy, total momentum, center of mass, and natural behavior in the flow direction cause eight exponents to disappear. For the numerical computation of Lyapunov spectra of differentiable dynamical systems, the method of Benettin *et al.* [13,14] is standard. By linearizing the equations of motion the time evolution of a complete set of tangent vectors can be expressed as

$$\dot{\boldsymbol{\delta}}_l(t) = M(\boldsymbol{\Gamma}(t))\,\boldsymbol{\delta}_l(t) + O(\boldsymbol{\delta}_l^2(t)) \quad (l = 1, \ldots, 6N), \tag{5}$$

where $M(\boldsymbol{\Gamma}(t)) = \partial \boldsymbol{G}(\boldsymbol{\Gamma}(t))/\partial\boldsymbol{\Gamma}(t)$ is the stability matrix and $\boldsymbol{\delta}_l(t)$ is the infinitesimal tangent vector between the reference trajectory and the perturbed trajectory. $6N$ $\boldsymbol{\delta}_l(t)$ vectors consist of basis vectors of the tangent space.

The time evolution of the hard-sphere system in tangent space involves hard elastic collisions of particles. To take these collisions into account, a generalization of Benettin's method is required. Briefly, the hybrid method of ordinary differential equations and discrete maps was developed by Dellago and Posch [15] to describe hard-sphere dynamics. The time evolution of the complete set of tangent vectors for hard-sphere systems is

$$\boldsymbol{\delta}_l^f = \frac{\partial F}{\partial \boldsymbol{\Gamma}}\cdot\boldsymbol{\delta}_l^i + \left(\frac{\partial F}{\partial \boldsymbol{\Gamma}}\cdot\boldsymbol{G}(\boldsymbol{\Gamma}^i) - \boldsymbol{G}(F(\boldsymbol{\Gamma}^i))\right)\delta\tau_l^c, \tag{6}$$

where $\delta\tau_l^c$ is the time delay between collisions in the reference system and in a satellite system displaced by $\boldsymbol{\delta}_l$. $\partial F/\partial\boldsymbol{\Gamma}$ is the matrix of the derivative of F. For a detailed description of the model and the computational techniques, we refer the reader to Ref. [15] for hard spheres and Refs. [1,2] for soft spheres.

The Lyapunov exponents are obtained from

$$\lambda_l = \lim_{t\to\infty}\frac{1}{t}\ln\left(\frac{|\boldsymbol{\delta}_l(t)|}{|\boldsymbol{\delta}_l(0)|}\right), \quad (l = 1, \ldots, 6N). \tag{7}$$

According to the Pesin formula [16], KS entropy h_{KS} is defined as the sum of all positive Lyapunov exponents in a closed system,

$$h_{\mathrm{KS}} = \sum_{\lambda_i > 0}\lambda_i\,. \tag{8}$$

The calculation of the Lyapunov exponents is the most time-consuming step, so we considered a system of 32 atoms moving in a rectangular periodic box for this calculation. The question of particle-number dependence of KS entropy per particle still remains to be answered. However, our calculations for the soft-potential case show that the differences in the values of h_{KS}/N are negligible between a system with $N = 32$ and one with $N = 64$. For example, at $\rho = 0.92$, $h_{\mathrm{KS}}/N = 5.08$ for both $N = 32$ and $N = 64$. The computations for the hard-sphere system are much more efficient, so we adopted $N = 64$ for the calculation of the Lyapunov exponents. We also confirmed that for hard spheres the value of h_{KS}/N shows no difference between the results for the systems with $N = 64$ and $N = 108$, as observed by van Beijeren *et al.* [17].

To obtain the self-diffusion coefficient D, the Green-Kubo formulation [18–20], expressed as the integrated velocity autocorrelation function (VACF), was used

$$D=\lim_{N\to\infty}\lim_{t\to\infty}\int_0^t C(\tau;N)\,d\tau, \tag{9}$$

where $C(\tau;N)=\Sigma_{i=1}^{N}\langle \boldsymbol{v}_i(0)\cdot\boldsymbol{v}_i(\tau)\rangle/3N$, with $\boldsymbol{v}_i(t)$ a velocity of a given particle. Due to the periodic boundary conditions imposed in the simulation, the size dependence of the VACF over the finite range of dynamical time accessible in the calculations was rather strong. The relatively small number of particles N does not allow the coexistence of the two phases, and the system is in either the solid or liquid phase. Furthermore, the periodic boundary conditions enhance the formation of the solid phase. If each simulation starts from a regular configuration with the particles arranged on a fcc lattice (simulation A), the formation of the solid phase is more likely to occur in the two-phase region. On the other hand, if the simulation starts with an initial configuration obtained by cooling the fluid state of higher temperature (simulation B), an extension of the fluid branch toward higher density would be expected. We performed both simulations A and B with $N=500$. The self-diffusion coefficients obtained from simulation A suddenly dropped to essentially zero from $\rho=0.92$, because of the early formation of a solid structure enhanced by the periodic boundary conditions. On the other hand, those obtained from simulation B changed smoothly as ρ increased beyond 0.92, showing that the system was still in a fluid state. Thus, simulation B is more suitable to reduce possible size effects, especially near the phase boundary when the simulation is performed with a relatively small number of particles. As expected, the numerical values of D (obtained from simulation B) for hard spheres showed a perfect match with those found by Alder, Gass, and Wainwright (AGW) [21], since both are based on molecular dynamics (MD) calculations for systems of 500 particles. But the values of D for the soft-sphere system with the WCA interaction potential were consistently above the estimates by AGW; this seems to be attributable to the fact that the effective diameter for the soft sphere defined as the first maximum of the $g(\sigma)$ was overestimated. Recent work by Erpenbeck and Wood (EW) [10] extended the AGW study with respect to system-size dependence and the long-time tail effect of VACF, and presented an improved formula for the self-diffusion coefficient. In Fig. 1, the calculated self-diffusion coefficients for hard spheres and soft spheres with the WCA interatomic potential, normalized with respect to the Enskog-theory diffusion coefficient, are compared with the EW expression. The formula by Erpenbeck and Wood can be written as

$$D/D_E=1+0.003\,828\,013\rho^*+3.381\,828\,1\rho^{*2}+3.868\,772\rho^{*3}, \tag{10}$$

where D_E is the Enskog-theory transport coefficient, defined as

$$D_E=\frac{0.382\,11\sigma}{\rho^*\sqrt{\pi m\beta}g(\sigma)}. \tag{11}$$

Here ρ^* is the reduced density defined as $\rho\sigma^3$. The two results are not in exact accord, but they show the same trend, as seen in Fig. 1.

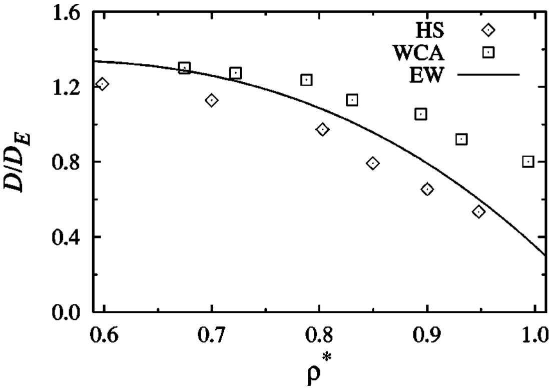

FIG. 1. Self-diffusion coefficient D, normalized with respect to the Enskog-theory diffusion coefficient D_E, as a function of density. Squares correspond to a soft-sphere system with WCA potential; diamonds correspond to a hard-sphere system (HS); the solid line is the empirical expression of the EW formula ($T^*=0.7$).

The value of D is sensitive to both the size and phase of the system, whereas the KS entropy per particle seems to be insensitive to both factors. Our numerical studies show that simulation B cannot generate the fluid phase for $\rho>0.9$ with $N=32$ due to the periodic boundary conditions. Instead, the final structures always result in periodic solid structures; corresponding self-diffusion coefficients become essentially zero due to the small system size. However, with $N=64$, simulation B can generate the liquid phase for $\rho=0.92$, and the corresponding value of D is 0.0201, which can be considered that of the liquid phase. Still, h_{KS}/N ($=5.08$) for $N=64$ is essentially identical to the value for $N=32$ ($h_{\mathrm{KS}}/N=5.08$; see Table I).

III. RESULTS AND DISCUSSION

For the system with WCA interaction potential corresponding to $n_g=6$ in Eq. (3), the KS entropy per particle h_{KS}/N shows a single maximum at $\rho=0.625$, and vanishes at very low or high density, whereas the KS entropy per particle divided by the average collision frequency shows a steady decrease as density increases. These results are con-

TABLE I. Numerical results for the KS entropy and the self-diffusion coefficients for the WCA potential and hard spheres (HS), obtained through simulation B.

WCA			HS		
ρ	h_{KS}/N ($N=32$)	D ($N=500$)	ρ	h_{KS}/N ($N=64$)	D ($N=500$)
0.5	6.74	0.202	0.5	7.88	0.203
0.6	7.15	0.142	0.5982	9.83	0.140
0.7	7.00	0.0920	0.6998	12.2	0.0901
0.8	6.33	0.0543	0.8028	15.0	0.0537
0.9	5.25	0.0273	0.8496	16.4	0.0389
0.92	5.08	0.0227	0.9002	18.3	0.0253
0.94	4.80	0.0189	0.9478	19.1	0.0172
0.96	4.51	0.0157			
0.98	4.19	0.0119			
1.0	3.85	0.00906			

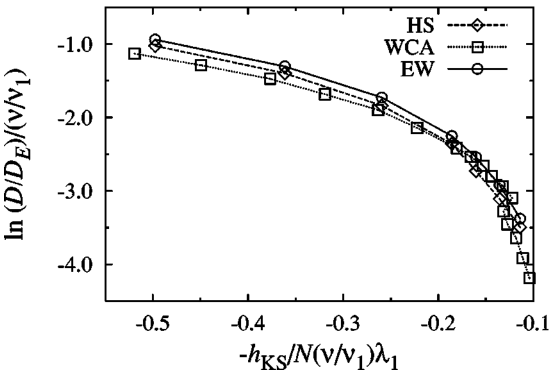

FIG. 2. The dimensionless self-diffusion coefficient defined as $D^* = (D/D_E)/(\nu/\nu_1)$ as a function of $h_{KS}/N(\nu/\nu_1)\lambda_1$. Diamonds and squares denote MD results for the hard-sphere (HS) and soft-sphere (WCA potential) systems, respectively; circles denote D values obtained from the EW formula ($T^* = 0.7$).

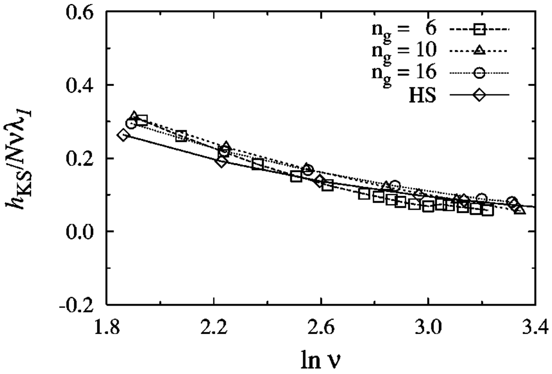

FIG. 3. $h_{KS}/N\nu\lambda_1$ as a function of average collision frequency ν. Diamonds represent data for the hard-sphere system; squares, triangles, and circles correspond to those for systems interacting via the soft potentials defined in Eq. (3) with $n_g = 6$, 10, and 16, respectively.

sistent with those presented by Dellago and Posch [4]. On the other hand, h_{KS}/N for the hard-sphere system increases steadily except at the point where the fluid-solid phase transition occurs, as shown in [4].

The Lyapunov exponents are local quantities in the sense that they depend on the dynamical events taking place in the system—namely, collisions—for which the velocities change. So it is reasonable to expect that there exists a general relationship between the Lyapunov exponents and the self-diffusion coefficients. In Fig. 2, we present the relationship between the self-diffusion coefficients and KS entropy for various densities. The diamonds and squares denote MD results for the hard- and soft-sphere systems, respectively; circles denote the D values obtained from the EW formula. To facilitate the comparison of the behavior for the systems of hard and soft spheres, we use the following dimensionless form for the self-diffusion coefficient and KS entropy: $D^* = (D/D_E)/(\nu/\nu_1)$, $h^*_{KS} = h_{KS}/N(\nu/\nu_1)\lambda_1$, where D_E is the Enskog-theory transport coefficient, ν is the average collision frequency, ν_1 is defined as $\nu_1 = 4(k_B T/\pi m \sigma^2)^{1/2}$, and λ_1 is the largest Lyapunov exponent. This figure demonstrates convincingly that there exists a universal relationship between D^* and h^*_{KS} that is valid for systems of both soft and hard spheres. This observation implies that atomic diffusion is a geometric phenomenon which can be uniquely accounted for by the frequency of binary collisions and KS entropy, representing a measure for the time rate of information loss and structural uncertainty. Specifically, throughout the range of density that corresponds to the liquid domain ($0.5 \leqslant \rho \leqslant 0.8$), the diffusion adheres to an Arrhenius-like behavior, which can be described by a simple scaling law. Table I shows the KS entropy per particle (h_{KS}/N) and the self-diffusion coefficients for systems of hard spheres and soft spheres with WCA interaction potential, obtained through simulation B for $0.5 \leqslant \rho \leqslant 1.0$. It is worth mentioning that the KS entropy values obtained from simulation A and those obtained from simulation B show no noticeable difference, even in the regime where the linear relationship breaks down.

Recently, van Beijeren and his colleagues [17] have shown both theoretically and analytically that a linear relationship holds between $h_{KS}/N\nu'$ and $\ln \nu'$ for hard-sphere systems at low density. They showed that the KS entropy per particle and per collision, when expanded with respect to density, becomes linear for a dilute gas in equilibrium,

$$h_{KS}/(N\nu') = a[-\ln(\nu'/\nu_1) + b] + O(\nu'^2), \tag{12}$$

where a is equal to 1 for the hard-sphere system. Notice that the definition of ν' in Ref. [17] is $4\rho\sigma^2(\pi k_B T/m)^{1/2}$, which differs from the average collision rate ν by the factor $g(\sigma)$. Our numerical results for the hard-sphere system show that the above linear relationship does not hold in densities corresponding to a liquid regime ($0.5 \leqslant \rho \leqslant 0.8$). However, if we use ν, which includes the average collision number $g(\sigma)$, instead of ν' in Eq. (12), then $h_{KS}/N\nu$ vs $\ln \nu$ shows a linear relationship with $a = 0.407$, even in the liquid regime ($0.5 \leqslant \rho \leqslant 0.8$). This suggests that the rate of information loss per collision is still uniquely related to the average collision rate with the same scaling law in a more generalized form, in which ν' is substituted for ν, even in the high density region. The relation becomes nonlinear in the region $0.8 \leqslant \rho \leqslant 1.0$, corresponding to the regime that precedes the formation of the solid. We extended the numerical study to systems with continuous interaction potentials and found that in $0.5 \leqslant \rho \leqslant 0.8$—which corresponds to the liquid regime—the linear relationship also holds, even though slope a becomes different from that of the hard-sphere system. For the potential defined in Eq. (3), we obtained the slope $a = 0.708$, 0.597, and 0.479, in the liquid regime for $n_g = 6$, 10, and 16, respectively, at $T^* = 0.7$. Thus, the slope approaches that of the hard-sphere system as n_g increases. This study shows that the linear relationship between the KS entropy and average collision rate still holds even for a system of soft spheres. This tells us that the rate of information loss can be uniquely accounted for by collision frequency in the region where the diffusion shows an Arrhenius-like behavior. If we further scale $h_{KS}/N\nu$ by λ_1, the largest Lyapunov exponent, and plot $h_{KS}/N\nu\lambda_1$ vs $\ln \nu$, we find that the same linear relationship can be applied to systems with different interaction potentials throughout the density range corresponding to the liquid domain, as shown in Fig. 3.

It is also instructive to view the dynamics of the tangent vectors in the subspaces associated with special degrees of freedom. In the present case, the tangent space is a simple product of configuration space R and corresponding momentum space P. Then the projection of the tangent vector $\boldsymbol{\delta}_l$ onto X space is $\boldsymbol{\delta}_{X,l} = \mathcal{P}(X)\boldsymbol{\delta}_l$, where $X = R$ or P. The projection operator $\mathcal{P}(X)$ can be represented as a diagonal matrix with element $\mathcal{P}_{\alpha\alpha}(X)$ equal to unity, if the α axis of $\boldsymbol{\delta}_l$ belongs to X, and equal to zero otherwise. We examined the behavior of the mean-squared X components of $\boldsymbol{\delta}_l$ as ρ varies, which is defined as $\delta^2_{X,l} = \langle \boldsymbol{\delta}_{X,l} \cdot \boldsymbol{\delta}_{X,l} \rangle$. Figures 4(a) and 4(b) show $\delta^2_{X,l}(X = P \text{ or } R)$ as functions of l for the hard-sphere and the soft-sphere (WCA potential) systems, respectively. Eight of the Lyapunov exponents vanish for reasons given in Sec. II ($93 \leqslant l \leqslant 100$); the corresponding $\delta^2_{X,l}$ components have no meaning, since Gram-Schmidt reorthonormalization has no ordering effect on the directions of their tangent vectors. On average, 96.2% of the squared length of $\boldsymbol{\delta}_1$ for hard spheres and 97.4% of that of $\boldsymbol{\delta}_1$ for soft spheres are contributed from the momentum subspace for $\rho = 0.5$; these numbers rise to 99.0% and 99.4%, respectively, for $\rho = 1.0$. This means that the instability of the phase-space trajectory is mostly accumulated in the momentum subspace in high density regions. For the same number density, the mean-squared P component of $\boldsymbol{\delta}_1$ for the soft-sphere system is higher than that of the hard-sphere system. We suggest that this is because the soft sphere has a larger effective diameter than the hard sphere. We also examined the structures of the pair correlation functions $g(r)$ obtained from simulation B for a wide range of densities. In the case of dilute gases ($\rho < 0.5$), local structural correlation expressed in terms of $g(r)$ is confined to the first-neighbor shell. As density increases, the range of the structural correlation becomes longer. It is interesting to note that the linear relation described by Eq. (12) breaks down when the structural correlation extends to the third-neighbor shell, which can be considered as the signature of the formation of the solid. Giaquinta and Giunta have shown that the liquidlike regime ($0.5 \leqslant \rho \leqslant 1.0$) can be divided into two regimes, depending on whether structural locking develops [22]. Our studies show that, in the liquidlike regime characterized by strong cooperativity ($0.5 \leqslant \rho \leqslant 0.8$), diffusion adheres to an Arrhenius-like behavior. A nonlinear type of relation holds in the regime ($0.8 \leqslant \rho \leqslant 1.0$) where structural locking develops, which corresponds to the regime that prepares the formation of a solid.

IV. CONCLUSIONS

In this paper, we studied the instability properties of phase-space trajectories for simple fluids in relation to self-diffusion. Detailed numerical analyses of the KS entropy and self-diffusion coefficient as a function of density indicate that the reduced self-diffusion coefficient in a dimensionless form $[D^* = (D/D_E)/(\nu/\nu_1)]$ has a unique relation with the dimensionless KS entropy per particle scaled by the largest Lyapunov exponent $[h^*_{\mathrm{KS}} = h_{\mathrm{KS}}/N(\nu/\nu_1)\lambda_1]$ by a simple scaling law: $D^* \propto \exp(h^*_{\mathrm{KS}})$. Next we examined the relationship between the KS entropy and average collision frequency for both systems of hard spheres and systems with continuous interaction potentials. The results demonstrate that $h_{\mathrm{KS}}/N\nu\lambda_1$ shows the same linear relationship with $\ln \nu$, even in systems with different types of pair potential. From analysis of the mean-squared X components of the tangent vectors, we also found that the major contributions to the instability of the phase-space trajectory come from the momentum variables for high density regions.

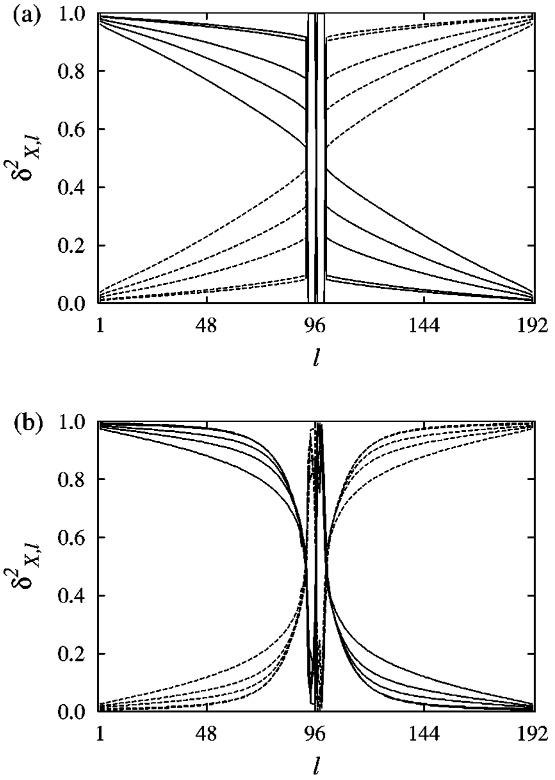

FIG. 4. Mean-squared X components $\delta^2_{X,l}$ as a function of the Lyapunov exponent index l for a hard-sphere fluid with 64 particles (a) and for a soft-sphere fluid with 32 particles (b), for various densities ranging from $\rho = 0.5$ to 1.0. The subspaces X are the momentum subspace P (solid lines) and the position subspace R (dashed lines).

ACKNOWLEDGMENTS

This research was supported by KRF, Korea-Germany Joint Project, 1998–2001.

---

[1] W.G. Hoover, H.A. Posch, and S. Bestiale, J. Chem. Phys. **87**, 6665 (1987).
[2] H.A. Posch and W.G. Hoover, Phys. Rev. A **38**, 473 (1988).
[3] Ch. Dellago, H.A. Posch, and W.G. Hoover, Phys. Rev. E **53**, 1485 (1996).
[4] Ch. Dellago and H.A. Posch, Physica A **230**, 364 (1996).
[5] W.G. Hoover and H.A. Posch, Phys. Rev. E **49**, 1913 (1994).
[6] D.J. Evans, E.G.D. Cohen, and G.P. Morriss, Phys. Rev. A **42**, 5990 (1990).
[7] M. Dzugutov, Nature (London) **381**, 137 (1996).
[8] M. Dzugutov, E. Aurell, and A. Vulpiani, Phys. Rev. Lett. **81**, 1762 (1998).

[9] R.J. Speedy, Mol. Phys. **62**, 509 (1987).
[10] J.J. Erpenbeck and W.W. Wood, Phys. Rev. A **43**, 4254 (1991).
[11] J. P. Hansen and I. R. McDonald, *Theory of Simple Liquids* (Academic Press, New York, 1976).
[12] V.I. Oseledec, Trans. Moscow Math. Soc. **19**, 197 (1968).
[13] G. Benettin, L. Galgani, A. Giorgilli, and J.M. Strelcyn, Meccanica **15**, 9 (1980).
[14] A. Wolf, J.B. Swift, H.L. Swinney, and J.A. Vastano, Physica D **16**, 285 (1985).
[15] Ch. Dellago and H.A. Posch, Physica A **240**, 68 (1997).
[16] Ja.B. Pesin, Sov. Math. Dokl. **17**, 196 (1976).
[17] H. van Beijeren, J.R. Dorfman, H.A. Posch, and Ch. Dellago, Phys. Rev. E **56**, 5272 (1997).
[18] R. Zwanzig, Annu. Rev. Phys. Chem. **16**, 67 (1965).
[19] M.S. Green, J. Chem. Phys. **22**, 398 (1954).
[20] R. Kubo, J. Phys. Soc. Jpn. **12**, 570 (1957).
[21] B.J. Alder, D.M. Gass, and T.E. Wainwright, J. Chem. Phys. **53**, 3813 (1970).
[22] P.V. Giaquinta and G. Giunta, Physica A **187**, 145 (1992).